Effect of Transition Metal Oxides on Optical and DC Conduction Mechanism of Zinc-Phosphate Amorphous Semiconducting Glass

[1,3]Souvik Brahma Hota , [2]Ashes Rakshit , [3]Debasish Roy,
[2]Debtanu Patra , [4,*] Dipankar Biswas

[1]Department of Mechanical Engineering, Techno India University, Bidhannagar, Salt Lake, Kolkata 700091, West Bengal, India.
[2]Department of Mechanical Engineering, Regent Education and Research Foundation, Barrackpore, Kolkata 700121, India
[3]Department of Mechanical Engineering, Jadavpur University. Kolkata-700032, India,
*[4, *]Department of Electronics & Communication Engineering, Regent Education and Research Foundation, Barrackpore, Kolkata 700121, India,*
Mail id: dipankar_aec@rediffmail.com

Abstract.

It has been investigated how the incorporation of transition metal oxides impacts on physical, electrical and optical characteristics of zinc phosphate glasses developed by the standard melt quenching method. Some nanophases ZnP_4O_{11}, $Zn_{2.5}MoVO_8$, $Zn[MoO_4]$ and MoV_2O_8 have been found to superimpose on amorphous glassy matrices. The acquired X-ray diffraction data have been used to determine the polycrystalline structure, crystallinity levels, and formed nanocrystallites's average size. UV-visible spectra of glass systems have been examined, which shows that the electronic transition is indirect. On the basis of their ultraviolet edges, the Optical Band Gap Energy and Urbach Energy have been estimated. The current glassy systems exhibit semiconducting characteristics, as evidenced by the non linear nature of DC conductivity and various activation energies at high and low temperatures. In addition, tiny polarons that hop via defect or localized sites are accountable for the DC conduction mechanism. Using Mott and Greaves variable range hopping models, DC conductivity has been explained.

Keywords. Glass nanocomposite; Optical Band gap; DC Conductivity; Mott's and Greaves model.

1. INTRODUCTION

In countless technological fields, including electronics, sensors, reflecting windows, optical filters, optical switches, and electro-optic devices, glass nanocomposites are being used extensively [1,2]. Addition of transition metal ions (TMI) leads to the structural and characteristics changes of glass nano-composites have recently been identified as promising research areas in non-linear optics. Due to their potential to yield several valence states, TMI incorporation in glass networks has been one of the methods used to create incredibly cheap luminous devices [3]. Due to their inherent ability in adopting many structural forms, such as octahedral, bipyramidal and polyhedral coordination environments in different oxidation states, vanadates have drawn a significant amount of attention. They have remarkable optical and electrical properties as a result of the compositions' formation of a V_2O_5 layered structure [4]. The V^{5+} ion is bonded in a VO_4^{3-} group with the number of four O^{2-} ions in tetrahedral symmetry, as seen by the structural behaviour of V_2O_5. The vanadate glass system's structure is composed of a layered chain of VO_4 polyhedron units [4]. Transition metal oxide (TMO) such as molybdenum trioxide modifies the structure of the glass instead of acting normally as a glass-forming oxide by merging octahedral MoO_6 or tetrahedral MoO_4 structural parts along with some other glass-forming oxides, as for example phosphorus pentoxide (P_2O_5), vanadium pentoxide (V_2O_5)etc. As Mo ions have existence in both the stable Mo^{6+} (accepter level) and Mo^{5+} (donor level) valence states and form MoO_4 tetrahedral units, the addition of MoO_3 can result in more packed glassy systems [5]. MoO_3-doped glasses made of phosphate have electro-optical characteristics that are advantageous for a number of technological applications [6].

On the other hand, zinc oxide (ZnO) modifies the sensitive features of the glass while also influencing its structure and stabilizing the glass network. In view of the fact that zinc cations in glassy materials can adopt both four and

six-fold coordination with oxygen ions, this is conceivable [7]. It is noteworthy that nanocomposites of ZnO-doped glass have excellent economical possibilities because they have wide application in many technological fields, including dielectric layers, varistors, and barrier ribs of plasma displays [7]. The process of hopping from the lower to the higher valence states can be initiated by portable charge carriers or tiny polarons, that can improve electrical transport characteristics of phosphate glasses doped with TMI. Doped glasses with two TMIs can achieve a super-exchange of electrons between redox ion pairs to a significant extent, or "hopping" which results in the non-linear features of activation energy [8]. Because of the combined transition metal-ion effect, this nonlinearity arises [9]. The electrical conduction process is influenced by the spreading of hopping distances of charge carrier or the electron's energy variances located at distinct potential wells as charged impurity atoms are present [10]. Additionally, variances in oxygen coordination or thermally induced structural vibrations cause variations in electrical conduction mechanism as well as the required activation energy for the conductivity procedure [10].

The initial goal of this study is the melt quench synthesis of three quaternary glassy systems with the formula $0.15P_2O_5$–$0.35ZnO$-$0.50(1-x)\ MoO_{3-x}V_2O_5$) Due to the existence of two TMOs, V_2O_5 and MoO_3, we are able to analyze the mechanism of DC conduction for quaternary glass systems with the nature of mixed transition ion effect. The exploration of the structural and optical absorption characteristics of glass systems using XRD(X-ray diffraction)and Ultraviolet-visible absorption methods are another significant focus of this work.

2. EXPERIMENTAL PROCEDURE

The unique chemical composition $0.15P_2O_5$–$0.35ZnO$-$0.50(1-x)MoO_3$-xV_2O_5) has been used to synthesize three quaternary glassy nanocomposite systems (x = 0.1, 0.2, and 0.3) with combined modifier oxides (MoO_3 and V_2O_5). ZnO, MoO_3, P_2O_5, and TeO_2 in the proper amount in powder form, all with 99% purity, have been methodically assorted in an alumina crucible according to the stoichiometry of each composition. The temperature of the high-temperature electrical furnace is then set to 150°C, and then, it rises at 10°C/min heating rate while the alumina crucible is placed inside the furnace. We cautiously notice the form of the assortment in the furnace every five minutes and record the temperature at which the composite melts. At temperatures between 770°C and 890°C, three samples of quaternary glass (x = 0.1, 0.2, and 0.3) are melted. The entire melt of each composition has been immediately cooled at a temperature of 25°C among two metal plates (superbly polished) in order to form translucent glassy specimens of 0.3-0.5 mm of thickness. To perform the structural measurement, the as-quenched solid glasses are converted into fine powdery form by grinding appropriately. The famous principle of Archimedes is used to find out the density of the as-prepared glass samples and acetone is used as the immersion liquid. The quaternary glass samples have been tested for density and molecular weight, which are then applied to calculate the molar volumes. An X-ray diffractometer has been used to examine the X-ray diffraction patterns using CuKα radiation with 1.541 Å of wavelength and a range of 10° - 80°, operating at 4° /min scanning rate with 0.02° step size. Glassy samples that have already been prepared are coated with high conductive silver paste on both sides in order to work as electrodes for electrical studies. With a high-precision LCR metre, the resistance of the silver-coated glass samples has been measured using the two-probe process at a range of temperatures between 60 and 550 °C.

3. RESULTS AND DISCUSSIONS

3.1. Investigation of Physical parameters

To determine the structural reforms nature in amorphous glassy or polycrystalline samples, density (ρ) is a fundamental feature or physical characteristic. Molecular weight, constituent element fraction, and glass structure type all have a significant impact on oxide glass density. The mean values of ρ of all glass specimens have been determined by well-known principle Archimedes (Eq. 1) by utilizing the following expression.

$$\rho = \left(\frac{W_{air}}{W_{air-W_{acetone}}}\right) \times \rho_{acetone} \quad (1)$$

$\rho_{acetone}$ refers to the density of the acetone (immersion liquid). While $W_{acetone}$ stands for the sample's weight when soaked in acetone and W_{air} refers to the glass sample's weight when suspended in air [11].

By applying the derived values of ρ, the following equation can be employed to determine the molar volume of individual sample [11].

$$V_M = \Sigma \frac{x_i M_i}{\rho} \quad (2)$$

In Eq. (2), x_i and M_i denotes the molar ratio and molecular weight of the i^{th} oxide, correspondingly.

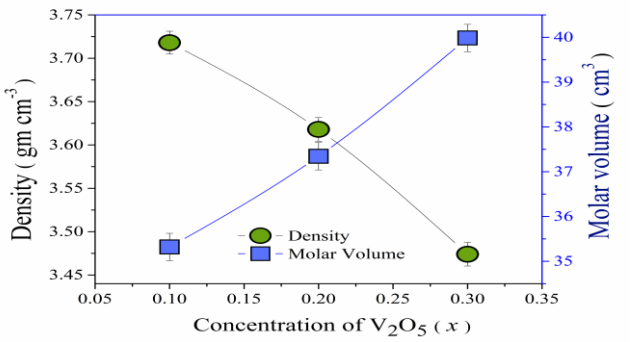

Fig. 1. Evaluated values of ρ and V_M

The alterations in ρ(density) and V_M (molar volume) values with deviations in concentration (x) of V_2O_5 are shown in Fig. 1, along with the typical inverse relationship between V_M (molar volume) and ρ(density). Because V_2O_5 has a greater molecular weight (181.88 g mol-1) than MoO_3 (143.94 g mol^{-1}) does, the composition formulation predicts that the molecular weight of all specimens increase as the V_2O_5 (x) concentration rises. Incorporating V_2O_5 into the glass-matrix thus works as a glass modifier, increasing the amount of non bridging oxygen (NBO) ions that in turn accelerates the dissociation of covalent bonds inside the network [12].

On the other hand, V_M (molar volume) has a strong correlation to the material's internal spatial organization. The variation in estimated V_M (molar volume) values as a function of the molar ratio of V_2O_5 is shown in Fig. 1. Less glass structure compaction results from the rising nature of V_M (molar volume), which also helps to increase bond length. By calculating the average values of V-V separation (d_{V-V}), it is possible to confirm that the reduced compaction of quaternary glass structures is caused by V_2O_5 inclusion.

The value of d_{V-V} has been assessed from the volume of 1-mol of V (V_M^V) and Avogadro's number (N_A) by the subsequent relationships.

$$d_{v-v} = \left(\frac{V_M^V}{N_A}\right)^{1/3} \quad (3)$$

Where,

$$V_M^V = \frac{V_M}{2(1-x_{V-ion})} \quad (4)$$

The $<d_{V-V}>$ value increases from 3.32 Å to 3.45 Å gradually with an increament in V_2O_5 concentration (x).Consequently, the decrement in density and the rising nature of Molar Volume for as-quenched nano-composites are actively supported by the effect of the presence of V_2O_5 considerably expanding the quaternary glass network.

3.2. Analysis of X-ray diffraction *Spectra*

The XRD patterns of V_2O_5 doped glass systems are exhibits in Fig. 2. The XRD patterns display sharp peaks with definite widths, which specify the crystallinity is there inside the amorphous translucent glass matrix. On the basis of this, it can be claimed that nanocrystallites(in a small number) are coinciding on the amorphous translucent glass matrix.

The subsequent relation determines the degree of crystallinity for every glassy system and the evaluated values are tabularized in Table 1.

$$\%\, Crystallinity = 100 \times \frac{Area\ of\ crystalline\ peak}{Total\ area\ under\ the\ patterns} \quad (5)$$

For the effect of the mixed modifier, it has been perceived that the percentage crystallinity values rise as more nanocrystallite phases emerge in zinc phosphate glass matrices. The available literature data has been used to identify and index the nanophases of specific diffraction peaks.

Table 1 demonstrates that the identified nanocrystallites of ZnP_4O_{11} [13], Zn [MoO_4] [14], $Zn_{2.5}MoVO_8$ (ICDD-50-1894) and MoV_2O_8 [15] are developed within the glassy matrix.

Using the Debye-Scherrer equation, the sizes of detected nanocrystallite (d_c) have been evaluated [16].

$$d_C = \frac{0.89\lambda}{\beta \cos\theta} \quad (6)$$

In Eq. (6), β symbolizes the full width at half maximum (FWHM), θ denotes the angle of Bragg diffraction, and λ refers to the wavelength (1.54 Å) of the Cu-Kα X-ray radiation employed. The evaluated d_c values for all three quaternary glasses are listed and tabulated in Table 1.

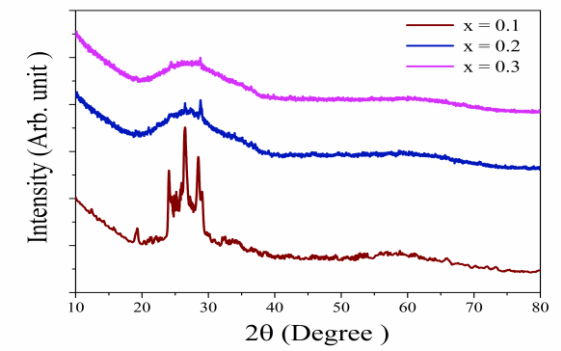

Fig. 2. XRD Spectra of all glasses

Table 1: Several estimated parameters from XRD spectra

Composition (x, mol%)	2θ (Degree) (±0.10)	FWHM	Nanocrystallite Phase	h	k	l	d_c (Average) (±0.06)	Crystalinity (%) (±0.05)
0.1	19.67	0.3234	ZnP_4O_{11}	1	2	-1	37.45	11.04
	24.11	0.1654	Zn [MoO_4]	0	1	2		
	26.54	0.1673	$Zn_{2.5}MoVO_8$	1	2	2		
	28.36	0.2621	MoV_2O_8	4	0	1		
0.2	26.54	0.1874	$Zn_{2.5}MoVO_8$	1	2	2	21.08	4.54
	28.36	0.2112	MoV_2O_8	4	0	1		
0.3	28.36	0.2321	MoV_2O_8	4	0	1	16.76	2.43

3.3. Analysis of UV-Visible Absorption Spectra

When analyzing structural alterations for optically influenced transitions and figuring out the optical direct or indirect bandgap energy of glassy amorphous systems, the spectra of optical absorption are essential [16]. The indirect transitions that emerge close to the band gap of the glassy structure have been observed and studied in order to accurately estimate the optical bandgap energy (E_{opt}) from the plotting of the photon energy (hv) and absorption coefficient (α) [16]. The following equation determines the value of E_{opt} from the UV-Vis electromagnetic waves absorption coefficient [16].

$$\alpha h\vartheta = \left[A\left(h\vartheta - E_{Opt}\right)\right]^m \quad (7)$$

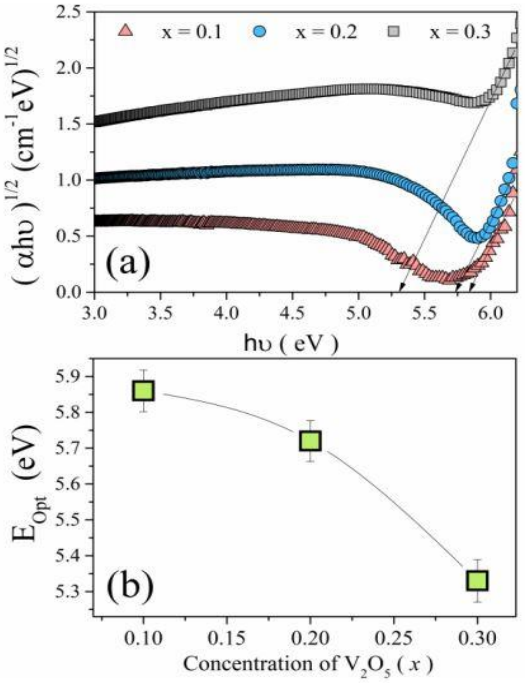

Fig. 3(a) Tauc's plot and **(b)** composition-dependent E_{Opt}

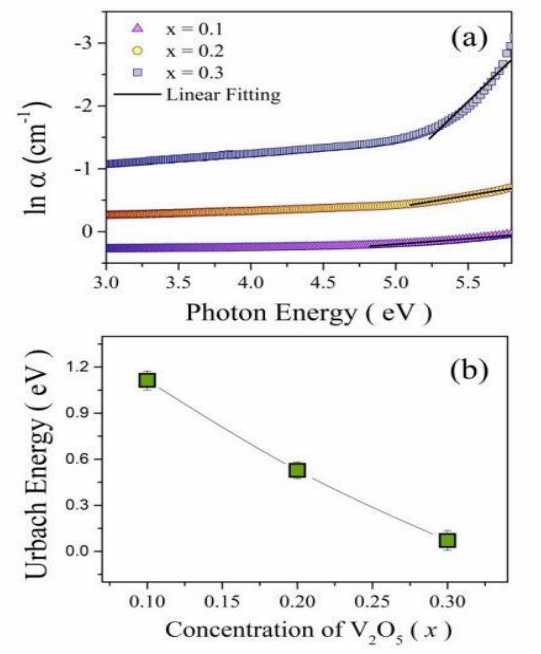

Fig. 4(a) ln α versus hυ and **(b)** composition-dependent E_U

Here, A stands in for the band tailing parameter's constant value. Depending on how the inter-band electronic movement behaves, the exponent (m) value is selected. Fig. 3(a) displays Tauc's plots of all the systems under study with the selective value of m is equal to 2 (for an indirectly permitted movement).

The values of E_{opt} of all glass nano-composite are revealed in Fig. 3(b). E_{opt} values of the quaternary systems drops with rising V_2O_5 content. All glass nanocomposite systems exhibit the same trend in the variation of E_{opt} and average size of nanocrystallite (d_C) (Table 2), i.e., the E_{opt} value is directly correlated with the d_C value.

The degree and nature of disorganization inside the glass-matrix are often correlated with Urbach Energy (E_U). The term "Urbach energy" (E_U) or "band tail energy" refers to the exponentially tailing portion of the non linear curve corresponding to absorption coefficient (ln α) vs hν that is situated near the optical bandgap. The values of the E_U are calculated by subtracting the slope's inverse from the linear fitting technique of the linear component in the lower photon energy section, as shown in Fig. 4 (a). The values of the E_U for each system of amorphous glass are calculated using the succeeding relation of Urbach's empirical rule.

$$\alpha = \alpha_0 \exp\left(\frac{h\upsilon}{E_U}\right) \quad (8)$$

Here, α_0 is used to symbolize the constant band tailing parameter. In Fig. 4(b), estimated values of composition-dependent Urbach energy (E_U) vs molar percentage of V_2O_5 (x) are revealed (b). With more V_2O_5 (x) presence, there are fewer defects, which resulted in narrower localised states, which in turn resulted in a reduced optical band gap. This decrease in Urbach energy indicates that defects are decreasing gradually.

3.4. Analysis of DC-Conductivity

Fig. 5 displays the temperature-dependent DC-conductivity of glass specimens. Fig. 5 shows the nonlinear nature of the σ_{dc} and how it increases with V_2O_5 content. Because the σ_{dc} is nonlinear, it is feasible that polarons or carriers with numerous equivalent activation energies are involved in the conduction mechanism [4]. The electron in the small polaron hopping process moves from one localized place to another [4].

The nonlinear curve can be separated into two discrete linear areas. With the assistance of the least square linear fit data, we estimated the activation energies of DC conductivity at low as well as high temperature areas, and Table 2 contains the results. The activation energy (E_{dc}) values for low and high-temperature DC conductivity are

found to decline as DC conductivity increases, which is strongly in accordance with the tiny polaron hopping theory [17].

The conduction's activation energy, and subsequently the DC conductivity, are influenced by the mean separation (R_V) between V^{4+} and V^{5+} ions during the hopping process. The conduction's activation energy, and the mean spacing (R_V) are highly correlated. The mean separation between V^{4+} and V^{5+} ions (R_V) can be determined from the association using $N_{V\text{-ions}}$ (V-ion concentration) from Eq. (9).

$$N_{V-ions} = \frac{mol\,\%\,of\,oxide \times N_A \times \rho}{Molecular\,weight\,of\,Composition\,(M)} \quad (9)$$

and,

$$R_V = \left(\frac{1}{N_{v-ion}}\right)^{\frac{1}{3}} \quad (10)$$

From Table 2, it can be shown that as $N_{V\text{-ions}}$ rise, R_V falls. As a result, more NBOs develop in the matrix of amorphous glassy system, σ_{dc} increases.The polaron radius (R_P), which has been determined using the R_V values, has been calculated using the relation shown below and is shown in Table 2.

$$R_P = \left(\frac{\pi}{6}\right)^{1/3}\left(\frac{R_V}{2}\right) \quad (11)$$

Table 2 shows that the radii of polarons decrease with increasing DC conductivity.

Table 2: Several estimated parameters associated with DC conduction mechanism

x (%)	E_{Low} (eV)	E_{High} (eV)	R_P (Å)	$N(E_{FM})$ x 10^{27} (eV^{-1}/cm^3)	$N(E_{FG})$ x 10^{26} (eV^{-1}/cm^3)
0.1	1.01	2.06	7.2	1.96	2.23
0.2	1.32	2.63	6.1	9.75	5.59
0.3	1.56	3.18	5.5	14.4	7.89

In the lower-temperature zone, a tiny polaron or charge carrier may hop from one localized site and another within the optical bandgap or mobility gap, in accordance with Mott's Variable Range Hopping (VRH) hypothesis. When the localized sites are accessible at the Fermi energy level and the density of states (DOS) is finite, Mott VRH takes place. The following equation represents the VRH conductivity mathematical formula [17].

$$\sigma_{dc} = A\,exp\left[-\left(\frac{T_0}{T}\right)^{0.25}\right] \quad (12)$$

The value of constant parameter T_0 is determined by the subsequent equation [17]

$$T_0 = \frac{16\alpha^3}{K_B N(E_{FM})} \quad (13)$$

Here, the DOS which is at the Fermi energy level inferred from Mott's VRH model is symbolized by $N(E_{FM})$, the localization distance of wave function of polaron is symbolized by α^{-1} and T_0 stands for the typical temperature. In Fig. 6 (a), DC-conductivity is displayed in proportion to $T^{-0.25}$ after the research outcomes are put into Eq. (12). The $N(E_{FM})$ values have been determined using Eq. (12) and the evaluated values are shown in Table 2 under the assumption that α^{-1} = 10 Å for localized sites and utilizing the slope of linear fit spectra (Fig. 6(a) solid red lines) have been taken into consideration. Table 2 demonstrates that $N(E_{FM})$ rises with composition. These findings demonstrate that the most important part of the conduction process is the rising concentration of V_2O_5 (x).

At temperatures above half the Debye temperature ($\theta_D/2$), the temperature dependency of the σ_{dc} data can't be justified by Mott's model. However, Greaves developed a dominating VRH model for this region temperature above ($\theta_D/2$) that is temperature-dependent. For the DC conductivity, Greaves proposed the following expression [17]:

$$\sigma_{dc}T^{0\cdot5} = A'\,exp\left[-\left(\frac{T_0'}{T}\right)^{0.25}\right] \quad (14)$$

The value of constant parameter T_0' is determined by the subsequent equation [17]

$$T_0' = \frac{19.4\alpha^3}{K_B N(E_{FG})} \quad (15)$$

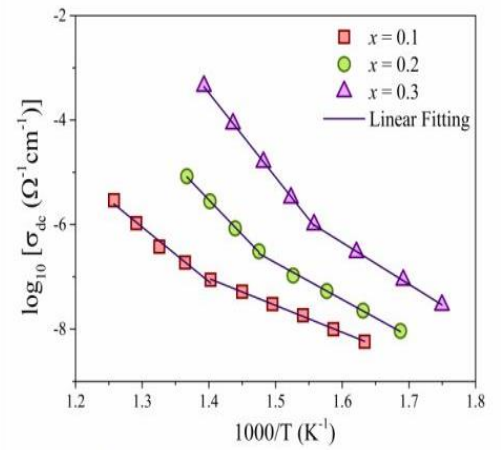

Fig. 5. DC conductivity with reciprocal temperature

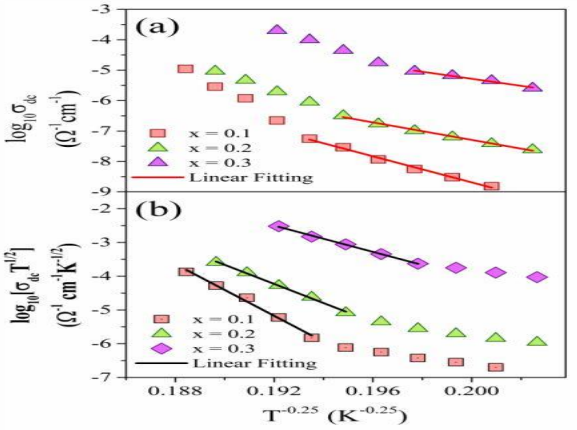

Fig. 6(a) Mott's VRH and **(b)** Greaves VRH model representation.

where $N(E_{FG})$ is the DOS at the Fermi level according to VRH model of Greaves. Fig. 6(b) shows a plot of log $(\sigma T^{1/2})$ against $T^{-0.25}$. Greaves' model is sufficient enough for meeting to the experimental results, as seen in Fig. 6(b). The values of $N(E_{FG})$ have been determined for the higher temperature zone using $\alpha^{-1} = 10$ Å for localized sites, the slopes of the linear best fit data in Fig. 6(b), and Eq. (14), and they are shown in Table 2. Additionally, $N(E_{FG})$ rises with composition (x), which is accordant with σ_{dc} once more.

4. SUMMARY AND CONCLUSIONS

Utilizing the melt of quenching process, three quaternary samples of glass nanocomposite with the chemical formulation $0.15P_2O_5$-0.35ZnO-0.50(1-x) MoO_3-xV_2O_5 with x values as 0.1, 0.2, and 0.3 have been developed. The formation of different-sized nanocrystallites that are superposed upon an amorphous glassy matrix is confirmed by XRD patterns. Due to structural changes, the assessed value of E_{opt} and E_U both decrease with increasing V_2O_5 content. The Urbach energy is declining, which means that more defect or localized sites have evolved inside the gap of mobility to support the mechanism of tiny polaron hopping. σ_{dc} shows non-linearity in its nature, that indicates semiconductor properties for all samples of glass nanocomposites. Additionally, the accumulation of V_2O_5 into the glass network alters the bond formation of the glass structure by enhancing the density of defect or localized sites. With more V_2O_5 present, the DOS at the Fermi level rises, improving conductivity, according to the investigation of σ_{dc} with Mott's and Greaves' model.

5. REFERENCES

[1] A. Bajaj, A. Khanna, B. Chen, J.G. Longstaffe, U.W. Zwanziger, J.W. Zwanziger, Y. Gómez, F. González, 'Structural investigation of bismuth borate glasses and crystalline phases', J. Non-Cryst. Solids, vol. 355, pp. 45–53, 2009.

[2] S. Bale, S. Rahman, 'Optical absorption and EPR studies on (70−x) Bi_2O_3–xLi_2O–30(ZnO–B_2O_3) (0 ⩽ x ⩽ 20) glasses', J. Non-Cryst. Solids, vol. 355, pp. 2127–2133, 2009.

[3] J. Meyer, S. Hamwi, M. Kröger, W. Kowalsky, T. Riedl, A. Kahn, 'Transition metal oxides for organic electronics: energetics, device physics and applications', Adv. Mater., vol. 24 (40), pp. 5408–5427, 2012.

[4] A.S. Das, D. Biswas, M. Roy, D. Roy, S. Bhattacharya, 'Effect of V2O5 concentration on the structural and optical properties and DC electrical conductivity of ternary semiconducting glassy nanocomposites', J. Phys. Chem. Solids, vol. 124, pp. 44–53, 2019.

[5] L. Bih, M. Elomari, J.M. Reau, M. Hadded, D. Boudlich, A.M. Yocaubi, A. Nadiri, 'Electronic and ionic conductivity of glasses inside the Li_2O–MoO_3–P_2O_5 system', Solid State Ion., vol. 132, pp. 71–85, 2000.

[6] G. Poirier, F.S. Ottoboni, F.C. Cassanjes, A. Remonte, Y. Messaddeq, S.J.L. Ribeiro, 'Redox behavior of molybdenum and tungsten in phosphate glasses', J. Phys. Chem. B, vol. 112, pp. 4481–4487, 2008.

[7] Allan B. Rosenthal, Stephen H. Garofalini, 'Structural role of zinc oxide in silica and soda-silica glasses', J. Am. Ceram. Soc., vol. 70 (11), pp. 821–826, 1987.

[8] S. Annamalai, R.P. Bhatta, I.L. Pegg, B. Dutta, 'Mixed transition-ion effect in the glass system: Fe_2O_3-MnO-TeO_2 ', J. Non-Cryst. Solids, vol. 358, pp. 1380–1386, 2012.

[9] I. Kashif, S.A. Rahman, A.A. Soliman, E.M. Ibrahim, E.K. Abdel-Khalek, A. G. Mostafa, A.M. Sanada, 'Effect of alkali content on AC conductivity of borate glasses containing two transition metals', Physica B, vol. 404, pp. 3842–3849, 2009.

[10] M.G. El-Shaarawy, 'Physical studies on ternary vanadium–phosphate glasses', J. Phys. Soc. Jpn., vol. 71 (4), pp. 1118–1125, 2002.

[11] A. S. Hassanien, I. Sharma, A.A. Akl, 'Physical and optical properties of a-Ge-Sb-Se-Te bulk and film samples: Refractive index and its association with electronic polarizability of thermally evaporated a-$Ge_{15-x}Sb_xSe_{50}Te_{35}$ thin-films", J. Non-Cryst. Solids, vol. 531, pp. 119853, 2020.

[12] I. Kashif, S.A. Rahman, A.A. Soliman, E.M. Ibrahim, E.K. Abdel-Khalek, A. G. Mostafa, A.M. Sanad, 'Effect of alkali content on AC conductivity of borate glasses containing two transition metals', Physica B, vol. 404, pp. 3842–3849, 2009.

[13] C.B. Doelle, D. Stachel, I. Svoboda, H. Fuess, 'Crystal structure of zinc ultra-phosphate, ZnP_4O_{11} ', Z. Kristallogr. Vol. 203, pp. 282–283, 1993.

[14] J. Meullemeestre, E. Penigault, 'Les molybdates neutres de zinc', Bull. Soc. Chim. Fr., vol. 10, pp. 3669–3674, 1972.

[15] P. Pailleret, J. Borensztajn, W. Freundlich, A. Rimsky, Structure crystalline de la phase MoV_2O_8, C.R. Seances Acad. Sci. Ser. C., vol. 263, pp. 1131–1133, 1966.

[16] D. Biswas, A.S. Das, R. Mondal, A. Banerjee, D. Deb, A. Dutta, S Bhattacharya, S Kabi, L S Singh, "Study of microstructure and electrical conduction mechanisms of quaternary semiconducting glassy systems: Effect of mixed modifiers", J. Non-Cryst. Solids, vol. 542, pp. 120104, 2020.

[17] D. Biswas, R.K.N. Ningthemcha, A.S Das, L.S. Singh, 'Structural characterization and electrical conductivity analysis of MoO_3–SeO_2–ZnO semiconducting glass nanocomposites', J. Non-Cryst. Solids, vol. 515, pp. 21–33, 2019.

Biographies

	**Souvik Brahma Hota** received the bachelor's degree in Aeronautical Engineering from Anna University in 2016, the master's degree in Mechanical Engineering from Techno India University in 2018, and the perusing philosophy of doctorate degree in Mechanical Engineering from Jadavpur University, respectively. He is currently working as a Faculty in the Department of Mechanical Engineering, Techno India University, West Bengal, India. His research areas include glass ceramics composites, electroless coating, surface technology, nano coating, micro alloying, material characterizations etc.
	**Ashes Rakshit** passed his B tech from Swami Vivekananda Institute Of Science and Technology. He passed his M.tech from Kalyani Government Engineering College. Currently he is working as an Assistant Professor in Department of Mechanical Engineering Regent Education and Research Foundation, Barrakpore, West Bengal, India. His research interest is composite materials.
	**Dr. Debasish Roy** received the bachelor's degree in Mechanical Engineering from University of North Bengal in 1986, the master's degree in Mechanical Engineering from Jadavpur University in 1989, and he persued philosophy of doctorate degree in Mechanical Engineering from Jadavpur University in 2004, respectively. He is currently working as a Professor in the Department of Mechanical Engineering, Jadavpur University, West Bengal, India. His research areas include fluid mechanics, hydro power, composite materials, glass ceramics etc.
	**Debtanu Patra** passed his B tech from Haldia Institute of Technology. He passed his M.tech from NITTTR , Kolkata. Currently he is working as an Assistant Professor in Department of Mechanical Engineering Regent Education and Research Foundation, Barrakpore, West Bengal, India. His research interests are Friction Stir Welding, composite materials etc.
	**Dr. Dipankar Biswas** is currently working as an Associate Professor in Department of Electronics & Communication Engineering, Regent Education and Research Foundation Barrackpore, West Bengal, India. Having completed his B.E. Degree from University of Burdwan, he started his journey of teaching and research since. Afterwards he completed his M.Tech. from WBUT. And while continuing his teaching and research obsession, he persuaded and got his PhD degree from National Institute of Technology Manipur**.** Now has more than 16 years of experience teaching in various engineering colleges. Alongside teaching, he has also been indulged in many high-quality researches producing more than 30 high original research articles in various international journals of high repute. His research areas include composite materials, chalcogenide glass, glass ceramics, glucose sensor etc.